# ISSUES IN NONLINEAR PARAMETER ESTIMATION AND MULTIVARIATE MODEL DISCRIMINATION: APPLICATIONS IN POLYMER REACTION ENGINEERING

THOMAS A. DUEVER*, ALEXANDER PENLIDIS*

In this paper an overview is given of issues in parameter estimation, model discrimination, and optimal sensor selection as they relate to the modelling of copolymerization processes. The problems are discussed in the context of a comprehensive polymerization simulation package that is being developed, which includes an extensive database. A brief desciption of the modelling equations together with a listing of equations used to predict copolymer composition, triad fractions and polymerization rate, which are the primary responses used throughout this paper, is given. The problem of reactivity ratio estimation is reviewed and a method based on the Error-in-Variables model (EVM) is described which has the advantage that it properly accounts for all the errors in the measurements being used in the estimation. Two methods for describing the uncertainty in the estimates obtained are given. The first establishes approximate elliptical contours which are approximate in both shape and size. The other approach offers an improvement in that contours having the correct shape are calculated. The problem of discriminating between two models based on the terminal and penultimate mechanism using the method proposed by Buzzi-Ferraris and Forzatti (1983) is described. Simulations using copolymer composition, triad fractions and copolymerization rate are compared. An experimental verification for styrene/methyl methacrylate and triad fraction data is discussed and contrasted with previous experimental results. A comparison between experiments designed using the model discrimination criterion and those using equally-spaced points shows that in general the designed experiments are better able to correctly discriminate. Furthermore, even in those cases when the equally-spaced experiments lead to correct model discrimination, they usually lead to poor estimates of the model prediction error and the parameter uncertainty. Finally, the problem of optimally selecting sensors for a polymerization process is discussed. The approach shown uses a Kalman filter to optimally combine the polymerization model with process data. The different sensor scenarios are ranked using the determinant of the state covariance matrix.

* Department of Chemical Engineering, University of Waterloo, Waterloo, Ontario, Canada N2L 3G1, e-mail: tduever@cape.uwaterloo.ca.

# 1. Introduction: Mathematical Modelling and Simulation Packages for Polymerization

Polymer reaction engineering is the combination of polymer science, chemistry and technology with process engineering principles. In the polymer reaction engineering spectrum, the fundamental phase consists of detailed investigations of polymerization reaction kinetics, guided by rigorous statistical experimental design techniques. On the other side of the spectrum, the applied phase consists of computer simulation and experimental studies of polymer reactor design, optimization, monitoring and control problems. The link between the fundamental and applied phases is mathematical modelling of polymerization systems, i.e., the effort to develop a repository of our understanding and knowledge of polymerization processes.

Mathematical models and their role in science and engineering are points of constant debate, especially when models are employed in an industrial environment. The role of a mathematical model is often misinterpreted. As a result, we frequently blame the model, instead of blaming our own lack of understanding about a process as well as our reluctance to experiment with a process in a meaningful and systematic way. Why then are models useful?

Models enhance our process understanding since they direct further experimentation. They act as a reservoir of one's knowledge about a process, and hence they may reveal interactions in a process that may be difficult, if not impossible, to predict solely from memory or experience, especially when many factors vary simultaneously. Since a model is a concise, compact form of process knowledge, models enhance transferability of knowledge; they may act eventually as an "inference engine", closely resembling the train of thought of an experienced human. In a sense, mathematical modelling is the best way to find out what one does not know about a process.

In developing the simulation package our efforts have been centred around the development of a general, flexible, user-friendly, computer simulation tool for the modelling of multicomponent bulk/solution/emulsion polymerization systems. Developing the modelling package is not an isolated effort; rather, we are committed to the long-term development in parallel of a comprehensive polymerization database for characteristics of monomers (currently the database includes fifteen widely used monomers), initiators, solvents, emulsifiers, chain transfer agents, inhibitors, rate constants, etc. This database is of course an integral part of the computer simulation package, as it constitutes the important link between polymerization kinetics and polymer reactor design.

The computer package is an extremely powerful tool for research, training and educational purposes. It guides and directs further experimentation, as there is a constant interplay between the experimental/parameter estimation phase and the simulation/extrapolation to new conditions/design of experiments phase. Extensions to "recipe design" situations and to tackling "what-if-type worst-case" scenarios are quite obvious. More details and additional package/database applications can be found in (Penlidis, 1994; Gao and Penlidis, 1996).

Despite revolutionary advances in both computer hardware and software, the problem of *bringing process data (knowledge) into a mathematical model in an optimal*

*fashion* remains. It is this aspect of the simulator development effort that we wish to discuss in this paper. This ultimately leads to issues in nonlinear parameter estimation and multivariate model discrimination, for example. In Section 2 the models used in this work will be introduced. Section 3 deals with the estimation of reactivity ratios which are key kinetic parameters used to model copolymerizations. In Section 4, we will summarize our work on model discrimination which combines simulations with experimental verification. Section 5 describes some of the results we have obtained in assessing the usefulness of different measurements using optimal sensor selection. We end the paper with some concluding remarks and future directions.

## 2. Copolymerization Models

As an example we will consider bulk copolymerization. A general reaction scheme which applies to this process would be made up of the following steps:

1. Initiator decomposition:

$$I \xrightarrow{k_d} 2R_{\text{in}}^{\bullet} \tag{1}$$

2. Reaction of primary radicals with monomer:

$$R_{\text{in}}^{\bullet} + M_1 \xrightarrow{k'_{p1}} R_{1,1}^{\bullet} \tag{2a}$$

$$R_{\text{in}}^{\bullet} + M_2 \xrightarrow{k'_{p2}} R_{1,2}^{\bullet} \tag{2b}$$

3. Primary radical termination:

$$R_{\text{in}}^{\bullet} + R_{n,ij}^{\bullet} \xrightarrow{k'_{t,ij}} P_n \tag{3}$$

4. Propagation:

$$R_{n,ij}^{\bullet} + M_k \xrightarrow{k_{ijk}} R_{n+1,jk}^{\bullet} \tag{4}$$

5. Transfer to monomer:

$$R_{n,ij}^{\bullet} + M_k \xrightarrow{k_{fM,ijk}} P_n + R_{1,k}^{\bullet} \tag{5}$$
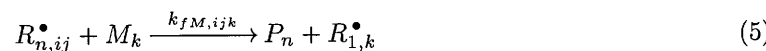
6. Branching reactions; transfer to polymer through:

(a) hydrogen abstraction:

$$R_N^{\bullet} + P_m \xrightarrow{k_{fP}} R_m^{\bullet} + P_n \tag{6a}$$

(b) terminal double-bond polymerization:

$$R_n^\bullet + P_m \xrightarrow{k_P^*} R_{m+n}^\bullet \tag{6b}$$

(c) internal double-bond polymerization:

$$R_n^\bullet + P_m \xrightarrow{k_P^{**}} R_{m+n}^\bullet \tag{6c}$$

7. Termination reactions:

$$R_{n,ij}^\bullet + R_{m,kl}^\bullet \xrightarrow{k_{t,ijkl}} P_{n+m} \text{ or } P_n + P_m \tag{7}$$
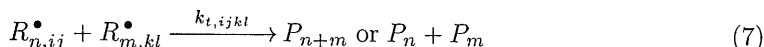
In this reaction scheme, $I$ refers to the initiator, $R_{in}^\bullet$ is the primary radical, $M_k$ is a monomer molecule of type $k$ ($k = 1$ or 2), $R_{1,1}^\bullet$ and $R_{1,2}^\bullet$ are radicals of length 1 ending in Monomers 1 and 2, respectively, $R_{n,ij}^\bullet$ are free radical chains of length $n$ ending in monomer units $ij$ ($i, j = 1$ or 2), $P_n$ is a polymer molecule containing $n$ monomer units and $R_n^\bullet$ is a free radical chain containing $n$ monomer units.

Based on this reaction scheme, the model is developed as a set of ordinary differential equations. The equations include a balance on the total moles of radicals, the moles of Monomers 1 and 2 being consumed, and the moles of monomer incorporated in the copolymer. The equations also include the change of conversion with time, the change in volume with time, the moments of the molecular weight distribution, and the change in the triad fractions with time. A listing of the equations and more details are given in (Burke, 1994).

In the above reaction scheme, the assumption has been made that penultimate reaction kinetics are applicable, whereby the next to last unit of the propagating polymer radical influences the reaction rate. As mentioned in the introduction, this is one of two prominent mechanisms which have been proposed to describe the propagation step. The other is the terminal mechanism, in which only the terminal unit of the propagating radical is thought to affect the rate. This leads to two different models, the terminal and the penultimate model. The problem of discriminating between the two will be discussed later. The propagation step in the terminal mechanism can be represented as

$$R_{n,i}^\bullet + M_j \xrightarrow{k_{ij}} R_{n+1,j}^\bullet \qquad i, j = 1, 2 \tag{8}$$
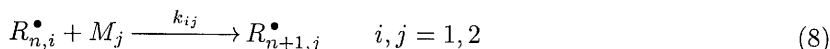
Although there are four propagation rate constants, $k_{ij}$, the rate is usually expressed in terms of the two homopolymerization rate constants $k_{11}$ and $k_{22}$ and two monomer reactivity ratios defined by

$$r_1 = \frac{k_{11}}{k_{12}}, \quad r_2 = \frac{k_{22}}{k_{21}} \tag{9}$$

The penultimate propagation step is represented by eqn. (4). The rate of polymerization is expressed in terms of two homopolymerization rate constants $k_{111}$ and $k_{222}$, four monomer reactivity ratios

$$r_{11} = \frac{k_{111}}{k_{112}}, \quad r_{21} = \frac{k_{211}}{k_{212}}, \quad r_{22} = \frac{k_{222}}{k_{221}}, \quad r_{12} = \frac{k_{122}}{k_{121}} \tag{10}$$

and two radical reactivity ratios

$$s_1 = \frac{k_{211}}{k_{111}}, \quad s_2 = \frac{k_{122}}{k_{222}} \tag{11}$$

It is interesting to note that the resulting terminal and penultimate models are nested; i.e., by setting $r_{11} = r_{21}$, $r_{22} = r_{12}$ and $s_1 = s_2$, the penultimate model equations can be reduced to those describing terminal kinetics.

Finally, in the subsections that follow, model equations will be summarized which predict some of the more common measurements which are made on the copolymer systems including copolymer composition, triad fractions and polymerization rate. For all the three responses, only the terminal model predictions will be reported. The equivalent penultimate model equations can be found in (Burke, 1994).

## 2.1. Copolymer Composition

The instantaneous copolymer composition $F_1$ (mole fraction of Monomer 1 in the copolymer) is given as a function of the monomer feed mole fractions $f_1$ and $f_2$ and the reactivity ratios $r_1$ and $r_2$ by

$$F_1 = \frac{r_1 f_1^2 + f_1 f_2}{r_1 f_1^2 + 2 f_1 f_2 + r_2 f_2^2} \tag{12}$$

Above small conversion levels, the change in feed composition with conversion, $x$, must be accounted for, as discussed by (Burke *et al.*, 1994a).

## 2.2. Sequence Distribution

Information about the structure of the copolymer in terms of the distributions of different sequences of monomer triads can also be predicted as a function of monomer feed compositions and reactivity ratios. Terminal model predictions of instantaneous Monomer-1 centred triad fractions $A_{ijk}$, where $i$, $j$ and $k$ refer to either Monomers 1 and 2, are given as

$$A_{111} = \frac{r_1^2 f_1^2}{r_1^2 f_1^2 + 2 r_1 f_1 f_2 + f_2^2} \tag{13a}$$

$$A_{211} = A_{112} = \frac{r_1 f_1 f_2}{r_1^2 f_1^2 + 2 r_1 f_1 f_2 + f_2^2} \tag{13b}$$

$$A_{212} = \frac{f_2^2}{r_1^2 f_1^2 + 2 r_1 f_1 f_2 + f_2^2} \tag{13c}$$

Model predictions for Monomer-2 centred triads are obtained by interchanging the subscripts for Monomers 1 and 2.

## 2.3. Copolymerization Rate

The terminal model prediction of the overall propagation rate is given as a function of the monomer feed composition, reactivity ratios and the homopolymerization rate constants $k_{11}$ and $k_{22}$ by

$$k_p = \frac{r_1 f_1^2 + 2 f_1 f_2 + r_2 f_2^2}{\dfrac{r_1 f_1}{k_{11}} + \dfrac{r_2 f_2}{k_{22}}} \tag{14}$$

Additional details on how the polymerization rate, $k_p$, is measured are given in (Burke *et al.*, 1995).

# 3. Reactivity Ratio Estimation

Reactivity ratios are key parameters which are required for designing, controlling and optimizing the performance of polymer reactors. Knowledge of the reactivity ratios allows for the prediction of copolymer composition, composition drift, sequence length distribution and polymerization rate as indicated by eqns. (12)–(14). These variables in turn are important in determining polymer properties and performance of the products made from the polymer. Reactivity ratios are usually estimated from low conversion ampoule experiments in which the assumption is made that no composition drift occurs and that the polymerization is in the chemically controlled regime. Data is then collected by measuring the copolymer composition, $F_1$ of copolymers made at several different initial feed compositions, $f_1$ and $f_2$. From this data the reactivity ratios can be estimated using eqn. (12). As pointed out by Rossignoli and Duever (1995) this model is nonlinear in the parameters and therefore requires an appropriate nonlinear estimation procedure. Behnken (1964) and Tidwell and Mortimer (1965) published approaches based on ordinary nonlinear least squares. Since the errors in measuring the polymerization feed composition $f_1$ and copolymer composition $F_1$ can be comparable, we prefer using the Error-in-Variables Model (EVM) in which errors in all of the measured variables are taken into account (Dube *et al.*, 1990; Rossignoli and Duever, 1995). Even though in the cases where the error in $F_1$ is much greater than $f_1$, nonlinear least squares is sufficient, we feel that EVM is the preferred approach. If nothing else, EVM forces the user to think about the errors present in all of the measurements made. Details of the implementation of EVM to the reactivity ratio estimation problem can be found in Rossignoli and Duever (1995).

Figure 1 shows the application of the EVM based estimation method to a simulated example involving the system styrene/methyl methacrylate, the data for which are shown in Table 3 of Rossignoli and Duever (1995). The triangle represents the true values used to simulate the data, while the circle represents the parameter estimates. Figure 1 also shows two different estimates of 95% joint probability contours which are used to quantify the uncertainty in the parameter estimates. The solid line depicts a relatively rough approximation to the joint posterior probability region for the estimated parameters, based on the assumption that the parameter estimates

are distributed as a multivariate normal, resulting in the elliptical posterior probability contour shown. Both the shape and probability content of this contours are approximate. The dashed line represents a somewhat better approximation to the joint posterior probability region. This approximation has the interesting property that it gives contours of correct shape (not in general elliptical), but approximate probability content. Equations for calculating these contours are given in Rossignoli and Duever (1995).

The design of reactivity ratio experiments was addressed by Tidwell and Mortimer (1970). They used the well-known D-optimality criterion to arrive at the following rules of thumb for approximating the design points:

$$f_{11} \cong \frac{2}{2 + r_1}, \quad f_{12} \cong \frac{r_2}{2 + r_2} \tag{15}$$

Using only these design points places a lot of trust in the validity of the model (eqn. (12)). If any doubt exists about the model, then additional design points should be added and some of these should be replicated to allow for lack of fit testing. Burke *et al.* (1993) have examined the problem of constrained designs. In the application of D-optimality, design points at the extreme conditions are often suggested. In copolymer systems, factors such as partitioning effects, phase separation or precipitation can often occur which interfere with the propagation step and lead to "apparent" reactivity ratios. Hence it is often desirable to constrain the design space to regions where these effects are not present.

## 4. Model Discrimination

When developing mechanistic models to describe processes, there are often several competing models. The question about which of the competing models is "best" and how the latter is chosen must then be addressed. Several models have been proposed to describe free-radical copolymerization, the most prominent of which are the terminal and penultimate models. In the past the approach taken to discriminate between these two models has been rather ad-hoc from a statistical point of view. Figure 2 shows a typical approach from the paper by Hill *et al.* (1982). Here ampoule experiments were performed equally spaced over the entire range of feed compositions to conversions of less than 5%. Copolymer composition was measured and used to estimate terminal and penultimate reactivity ratios using instantaneous composition equations. Since the terminal model and penultimate models are nested, an F-test was used to show if the added parameters in the penultimate model provided a significantly better fit of the data. These experiments do not seem to be optimal for either parameter estimation or model discrimination. In this section, an approach based on statistical model discrimination will be described. A summary of simulation and experimental results will be given. As well, a comparison between results based on equally-spaced experiments and those designed using model discrimination methodology will be described.
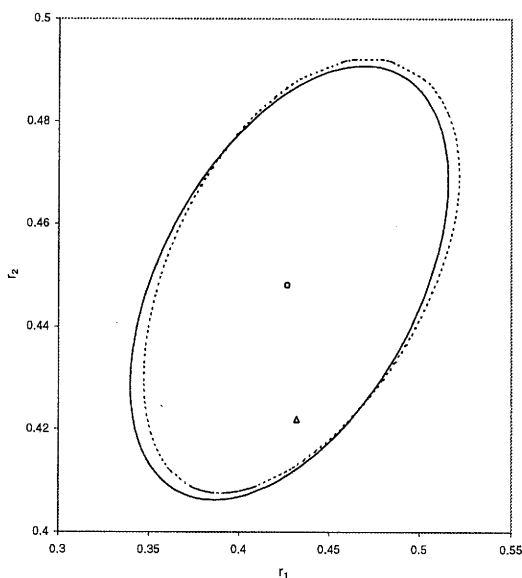
Fig. 1.  The 95% joint probability contour for the application of EVM to the esti-
         mation of reactivity ratios. The solid line represents the elliptical contour,
         while the dashed line represents the contour having the correct shape but
         approximate probability level. The "triangle" represents the true parameter
         values used to simulate the data, while the "circle" is the point estimate.
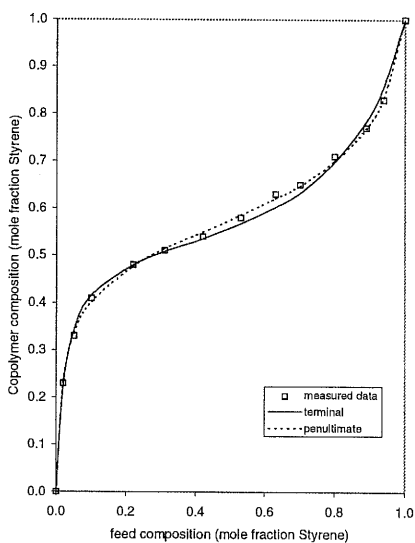


Fig. 2.  Copolymer composition data of Hill *et al.* (1982) for styrene/acrylonitrile.
         The solid line shows the fitted terminal model, while the dotted line shows
         the fitted penultimate model.

In the general model discrimination scenario, $m$ different models are proposed to describe a process:

$$y_i = f_i(x, \theta_i) + \varepsilon_i, \quad i = 1, 2, \ldots, m \tag{16}$$

where $y_i$ represents one or more responses, $x$ represents the independent variables used to describe the input conditions, $\theta_i$ are the parameters, $f_i$ is the $i$-th of $m$ candidate models and $\varepsilon_i$ is the error term. Model discrimination is a sequential procedure consisting of two steps:

- experimental design

- data analysis

applied in a sequential, iterative fashion. In the initial stage parameter estimates are obtained from the literature, past work, or by performing $n - 1$ preliminary experiments. One then performs the next ($n$-th) experiment for those values of $x$ identified by an appropriate model discrimination criterion, which locates where there are the largest differences between the model predictions.

In our work we compared three different criteria for model discrimination: the exact entropy approach by Reilly (1970), the approach published by Hsiang and Reilly (1971) and the method of Buzzi-Ferraris and Forzatti (1983). We compared these criteria with a simulation study involving three different copolymer systems and three different measurements or combination of measurements, namely copolymer composition (Burke *et al.*, 1994a), triad fractions (Burke *et al.*, 1994b) and rate and copolymer composition (Burke *et al.*, 1995). In these studies we also studied the effects of error level and quality of initial parameter estimates. Since the most promising of the discrimination methods we looked at was that of Buzzi-Ferraris and Forzatti (BFF) a summary of the simulation and experimental verification results for this method will be presented.

The BFF criterion chooses the $n$-th model discrimination experiment by maximizing the criterion given by:

$$T(x_n) = \frac{\sum\limits_{i=1}^{m-1} \sum\limits_{j=i+1}^{m} (\hat{y}_i - \hat{y}_j)^2}{(m-1)\left(ms^2 + \sum\limits_{i=1}^{m} s_i^2\right)} \tag{17}$$

where $s^2$ is an estimate of the experimental error variance and $s_i^2$ is an estimate of the prediction variance for the $i$-th model. The multivariate extension of this criterion is reported in Burke *et al.* (1994b). The criterion has the desirable property that if $T < 1$ for all $x_n$, then no discrimination is possible and either more parameter estimation experiments are needed or all of the candidate models are equally good descriptions of the process. Since the criterion in eqn. (17) is a simple ratio of the variance in the difference between predictions to the average variance in the predictions, and since the models are nested, the models can be compared using an $F$-test:

$$F = \frac{(\text{SSR}_2 - \text{SSR}_1)\big|(k_1 - k_2)}{\text{SSR}_1\big|(n - k_1)} \tag{18}$$

where $SSR_1$ and $SSR_2$ are the sums of squared residuals for both models calculated from the regression analysis, and $k_1$ and $k_2$ are the number of parameter values in each model, respectively. The $F$ value calculated in (18) is then compared to the $F$-distribution with $k_1 - k_2$ and $n - k_1$ degrees of freedom to determine whether the extra parameters in Model 1 provide a significantly better fit to the data.

## 4.1. Copolymer Composition

For each of the three copolymer measurements considered, the effects of three variables including measurement error level, initial parameter estimates and the model used to generate the simulated data, were studied by simulation. The experimental design for each simulation run is shown in Table 1. This design was repeated for each of the three copolymer systems considered (styrene/methyl methacrylate, styrene/acylonitrile and styrene/butyl acrylate) to determine if the nature of the copolymer system itself had any effect. Each simulation run (row in Table 1) simulated up to 20 experiments, consisting of initial parameter estimation experiments and sequential model discrimination experiments.

Figure 3 shows the outcome of a typical simulation run (run 13 from Table 1). The system and conditions studied here are comparable to those used in the study of Hill *et al.* (1982) depicted earlier in Fig. 2. It is interesting to note that discrimination was possible here using half the number of experiments reported by Hill *et al.*

Tables 2 a–c summarize the results for all three copolymer systems studied. For each "Simulation Model" there are a total of nine cases corresponding to the three initial parameter estimate values and the three error levels. When the strong penultimate model was used to simulate the data, it was correctly identified in greater than 80% of the cases, while a weak penultimate effect was correctly identified in over 60% of the cases.

Problems did arise at the high error level. This level was incidently much higher than typical errors reported in the literature. The problem here manifested itself not in the choice of the wrong model, but rather in neither model being chosen. The choice of the correct model was also more difficult for the system styrene/butyl acrylate, where one of the reactivity ratios is close to unity. Some overfitting by the penultimate model was observed leading to incorrect selection of the penultimate model when in fact the terminal model was the correct one. Overfitting leads to an experimental error variance estimate obtained from the penultimate model, $s^2_{\text{penultimate}}$, which is much smaller than the experimental error variance, $\sigma^2$. This problem was corrected by running independent replicates to establish the error variance. Overall variation in the quality of the initial parameter estimates had very little effect on the selection of the correct model.

The results of the simulation study based on composition data demonstrated that composition data provides more information for the purpose of discriminating between the penultimate and terminal models than had previously been thought. Furthermore, it was possible to determine smaller penultimate effects. Finally, the use of statistical model discrimination can assist in minimizing the number of experiments necessary to identify the correct model, compared to previous approaches.

Table 1.  Experimental design for simulation runs.

| Run | Simulation Model | Initial Reactivity Ratio Estimates | Error Level |
|-----|------------------|-----------------------------------|-------------|
| 1 | Terminal | Poor | Low |
| 2 | Terminal | Poor | Medium |
| 3 | Terminal | Poor | High |
| 4 | Terminal | Neutral | Low |
| 5 | Terminal | Neutral | Medium |
| 6 | Terminal | Neutral | High |
| 7 | Terminal | Good | Low |
| 8 | Terminal | Good | Medium |
| 9 | Terminal | Good | High |
| 10 | Strong Penultimate | Poor | Low |
| 11 | Strong Penultimate | Poor | Medium |
| 12 | Strong Penultimate | Poor | High |
| 13 | Strong Penultimate | Neutral | Low |
| 14 | Strong Penultimate | Neutral | Medium |
| 15 | Strong Penultimate | Neutral | High |
| 16 | Strong Penultimate | Good | Low |
| 17 | Strong Penultimate | Good | Medium |
| 18 | Strong Penultimate | Good | High |
| 19 | Small Penultimate | Poor | Low |
| 20 | Small Penultimate | Poor | Medium |
| 21 | Small Penultimate | Poor | High |
| 22 | Small Penultimate | Neutral | Low |
| 23 | Small Penultimate | Neutral | Medium |
| 24 | Small Penultimate | Neutral | High |
| 25 | Small Penultimate | Good | Low |
| 26 | Small Penultimate | Good | Medium |
| 27 | Small Penultimate | Good | High |

Table 2.  Application of the Buzzi-Ferraris method using composition data.

| Simulation Model | Model Chosen as Best at 95% Confidence (number of simulation runs) | | |
|---|---|---|---|
| | Terminal | Penultimate | Neither |
| 2a Application to styrene/methyl methacrylate | | | |
| Terminal | 4 | 1 | 4 |
| Strong penultimate | 1 | 7 | 1 |
| Small penultimate | 1 | 5 | 3 |
| 2b Application to styrene/acrylonitrile | | | |
| Terminal | 2 | 2 | 5 |
| Strong penultimate | 0 | 9 | 0 |
| Small penultimate | 1 | 6 | 2 |
| 2c Application to styrene/butyl acrylate | | | |
| Terminal | 1 | 1 | 7 |
| Strong penultimate | 2 | 6 | 1 |
| Small penultimate | 1 | 5 | 3 |

## 4.2. Triad Fractions

As indicated in eqn. (13), copolymer triad fractions depend upon the same reactivity ratios as copolymer composition. In fact, they are simulated using the same models as copolymer composition. One characteristic which is important to note for the purpose of parameter estimation is that Monomer-1 and Monomer-2 centred triad fractions sum to unity respectively, i.e.,

$$A_{111} + A_{112+211} + A_{212} = 1 \tag{19a}$$

$$A_{222} + A_{221+122} + A_{121} = 1 \tag{19b}$$

It is well-known that when multiple responses exhibit collinearity, as the triad fractions do here, this can have adverse effects on the stability of the parameter estimates obtained. The solution here is to use only four of the six triad fractions. This was accomplished here by removing that triad fraction from each group which had the smallest measured value. Parameter estimation is accomplished using the determinant criterion introduced by Box and Draper (1965).

The results for the three systems are summarized in Tables 3 a–c. In comparison with the composition results shown in Table 2, in almost every case the correct model

Table 3. Application of the modified Buzzi-Ferraris method using triad fraction data.

| Simulation Model | Model Chosen as Best at 95% Confidence (number of simulation runs) | | |
|---|---|---|---|
|  | Terminal | Penultimate | Neither |
| 3a Application to styrene/methyl methacrylate | | | |
| Terminal | 9 | 0 | 0 |
| Strong penultimate | 0 | 9 | 0 |
| Small penultimate | 0 | 9 | 0 |
| 3b Application to styrene/acrylonitrile | | | |
| Terminal | 9 | 0 | 0 |
| Strong penultimate | 0 | 9 | 0 |
| Small penultimate | 0 | 9 | 0 |
| 3c Application to styrene/butyl acrylate | | | |
| Terminal | 8 | 0 | 1 |
| Strong penultimate | 0 | 9 | 0 |
| Small penultimate | 0 | 9 | 0 |

was identified. The use of triad fractions therefore greatly improved our ability to correctly discriminate compared to composition data (the correct model was picked in greater than 98% of the simulations). This improvement is due to the use of four triad fractions instead of just one copolymer composition measurement.

## 4.3. Copolymerization Rate

The penultimate model for predicting copolymerization rate (eqn. (14)) contains eight parameters including four reactivity ratios (eqn. (10)), two radical reactivity ratios (eqn. (11)), and two homopolymerization propagation rate constants, $k_{111}$ and $k_{222}$. When an attempt was made to estimate all eight parameters using only rate data, the estimates obtained were highly correlated and unstable, indicating that by themselves, rate data do not contain sufficient information. To obtain better parameter estimates, rate data were combined with copolymer composition data, which reduced the correlation in the estimates. When rate and copolymer composition were combined, the results as far as model discrimination are concerned are similar to those obtained for triad data (Burke *et al.*, 1995).

## 4.4. Experimental Verification

Having studied the penultimate/terminal model discrimination problem by simulation, an experimental verfication study was carried out. Low conversion ampoule experiments were carried out using the styrene/methyl methacrylate copolymer system. This system was chosen since it is of considerable academic interest and contradictory results have been reported in the literature about the presence of a penultimate effect.

In the first phase, eight parameter estimation experiments were carried out, which consisted of two independent replicates of the four optimal compositions which were identified using a multiresponse D-optimality criterion similar to that reported by Draper and Hunter (1966). Triad fraction data was then collected using $^{13}$C-NMR with peak assignments as reported in the literature by Aerdts (1993).

Figure 4 shows the joint 95% confidence region for the terminal model reactivity ratios. This contour defined by eqn. (4) of (Burke $et\ al.$, 1996) has the correct shape but approximate probability level and represents a significant improvement over the elliptical approximation which can be obtained based on a linearization of the model and standard linear regression theory. Figure 5 shows a confidence contour calculated for parameter estimates calculated from a set of triad fractions for the same copolymer system using the same number of experiments reported by Maxwell $et\ al.$ (1993). Comparison of the two plots demonstrates the effect of the experimental design used. In the Maxwell $et\ al.$ data set, very few experiments were carried out at high styrene content and therefore $r_2$, the reactivity ratio for methyl methacrylate, is estimated much more precisely than $r_1$ the reactivity ratio for styrene. In fact, the open contour indicates that the estimate of $r_1$ is indeterminate.

In Phase 2 of the investigation, the multivariate analog of the BFF criterion was used to design the first model discrimination experiment. However, over the entire monomer feed composition, the design criterion $T$ was less than $p$, the number of independent measurements or responses available from an experiment. As with the single response case, when $T < p$, this is an indication that model discrimination is not possible. The fact that the maximum of the criterion value was less than $p$ indicates that either the two models are equivalent or that additional parameter estimation experiments are necessary to reduce the variance of the parameter estimates and hence the model predictions. Therefore an additional estimation experiment was designed using the $G$-optimality criterion, which choses an experiment to minimize the maximum prediction variance, or in the multiresponse case the trace of the prediction covariance matrix.

Figure 6 shows the joint confidence region obtained after addition of the ninth experimental point. By comparing with Fig. 4, it is evident that the addition of a single additional experiment has caused a dramatic reduction in the uncertainty of the terminal model parameter estimates. Figure 7 shows the marginal joint confidence region for the penultimate parameters $r_{11}$ and $r_{21}$. Note that the terminal model line $r_{11} = r_{21}$ passes through the joint confidence region slice. This together with the appropriate $F$-test indicates that there is no significant improvement obtained here in describing the data by using the penultimate model and hence the terminal model appears to be an adequate representation of the data. Additional details on the experimental verification can be found in Burke $et\ al.$ (1996).
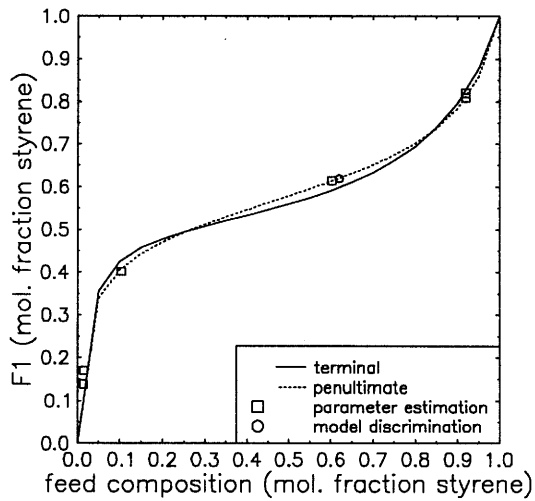
Fig. 3. This plot is an example of the simulation results for the application of the Buzzi-Ferraris method to the system styrene acrylonitrile (run 13 from Table 1). The squares are parameter estimation experiments designed using the D-optimal criterion. The circle is the model discrimination experiment designed using the Buzzi-Ferraris method.
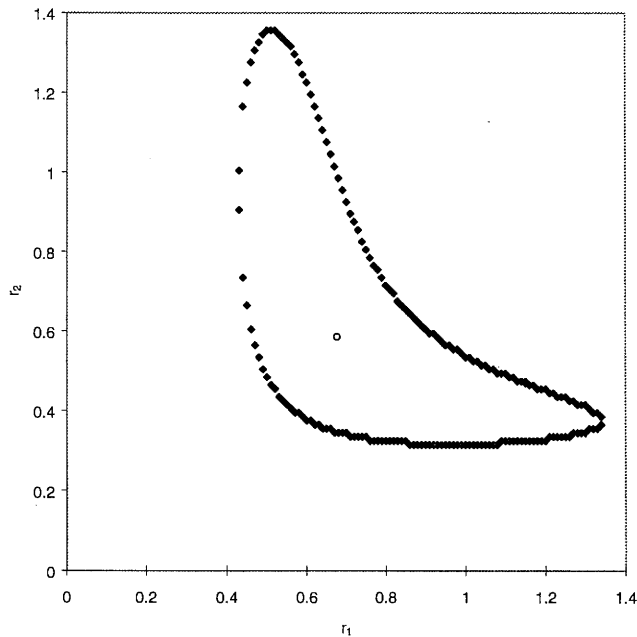


Fig. 4. The 95% joint confidence region for the terminal model parameters after eight experiments. The 'o' represents the point estimates.
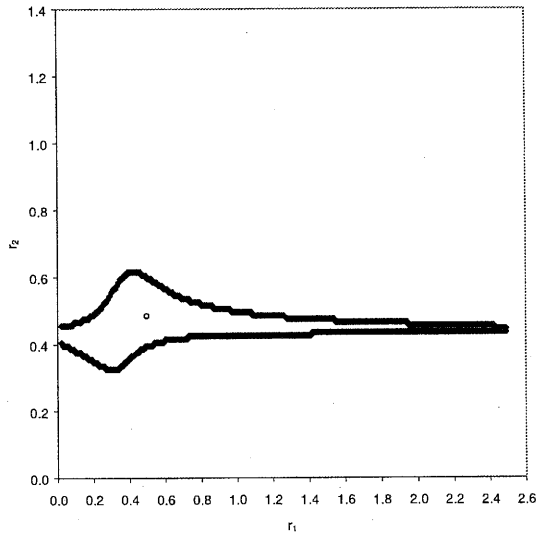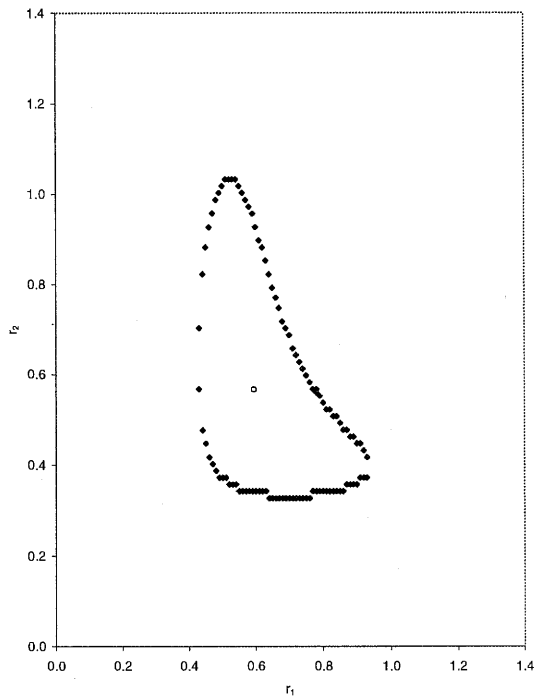
Fig. 5. The 95% joint confidence region for the terminal model parameters based on the data of Maxwell *et al.* (1993). The 'o' represents the point estimates.



Fig. 6. The 95% joint confidence region for the terminal model parameters after nine experiments. The 'o' represents the point estimates.

## 4.5. Equally-Spaced Data

Earlier on, in discussing Fig. 2 which shows the data collected by Hill *et al.* (1982), it was pointed out that a common approach is to space experiments evenly over the entire composition range. The data shown in Fig. 2 are based on a total of 14 experiments. Figure 3 shows the results of a simulation run carried out under conditions similar to those used to collect the data in Fig. 2. It was noted that using the statistical model discrimination approach only 7 experiments were necessary to correctly select the penultimate model, hence indicating that fewer experiments could be used. However, this comparison is not entirely fair and begs the question: could 7 equally-spaced experiments also correctly identify the "true" model? To answer this question an additional set of simulation experiments was run, in which equally-spaced experiments were carried out under identical conditions to those using the BFF criterion. In addition, exactly the same number of experiments was used. For example, Fig. 8 is the plot corresponding to Fig. 3 for the equally-spaced case. In both cases the same conditions were used: composition data, the strong penultimate model, low level of experimental error and neutral initial estimates. In this particular case, the analysis did show that the penultimate model was the best model for the system based on seven equally-spaced experiments. However, this was not the case for equally-spaced experiments in general.

Table 4 compares the results of the equally-spaced simulations with those obtained using the BFF model discrimination criterion. The experiments designed using the BFF method were better able to identify the correct model regardless of which "true" model was used to generate the data. Noticeable improvements were also made at all levels of experimental error and for all values of the initial reactivity ratios. In particular, the table shows that it is most crucial to use designed experiments when the terminal model is used to generate the data, when the error level is high, and when the initial reactivity ratio estimates are poor. It is important to point out that while this result is not unexpected, it corresponds to a very realistic scenario, in that when one carries out actual experiments, one is always faced with experimental error, one never knows which model is "true", and one can never know the accuracy of initial parameter estimates.

Table 5 shows the comparison between equally-spaced experiments and BFF designed experiments for triad fractions. In this case, equally-spaced experiments performed as well as those designed using BFF as far as choosing the correct model. However, an important point that came out of the comparison, is that differences did occur between the two approaches with respect to the accuracy and precision of the resulting parameter estimates. In all of the simulations involving designed experiments, there was independent replication of experiments. Given the low number of experiments relative to the number of model parameters, this use of replication should produce a better estimate of the experimental error variance than would be obtained by equally-spaced experiments. In fact, when the variance estimates were examined, it was found that equally-spaced experiments were much more likely to underestimate the true error covariance matrix. In the case of triad fraction data, based on regression of the terminal model, equally-spaced experiments produced lower esti-

Table 4.  Summary of simulations involving copolymer composition. Comparison of equally spaced experiments with those designed using the BFF method.

| True Model Chosen as 'Best' (% of simulations) | | |
|---|---|---|
| A. Based on Model Used to Generate the Data | | |
| True Model | Equally -spaced Experiments | Buzzi-Ferraris and Forzatti Method |
| Terminal | 7.4 | 25.9 |
| Strong penultimate | 48.2 | 81.5 |
| Small penultimate | 37.0 | 59.3 |
| All models | 30.9 | 55.6 |
| B. Based on the Level of Experimental Error | | |
| Error Level | Equally-spaced Experiments | Buzzi-Ferraris and Forzatti Method |
| Low | 37.0 | 63.0 |
| Medium | 40.7 | 63.0 |
| High | 14.8 | 40.7 |
| C. Based on the Initial Parameter Estimates | | |
| Initial Reactivity Ratios | Equally-spaced Experiments | Buzzi-Ferraris and Forzatti Method |
| Poor | 22.2 | 51.9 |
| Neutral | 40.7 | 48.1 |
| Good | 29.6 | 66.7 |

mates of the covariance matrix in 85% of the simulations. For the penultimate model this number was 82%. Therefore, even though equally-spaced experiments correctly identified the right model, the variability of the measurements was underestimated. Since the estimated error covariance matrix is used in the calculation of the covariance matrix for the estimated parameters, the variability of parameter estimates will also be underestimated.

## 5. Optimal Sensor Selection

As the discussion in Section 4 has revealed, the ability to discriminate between different models depends, at least to some extent, on the type of measurement used, i.e., better discrimination was achieved with triad fractions compared with copolymer composition for example. Furthermore we know that triad fraction data can lead to

Table 5. Summary of simulations involving triad fraction data. Comparison of equally spaced experiments with those designed using the BFF method.

| True Model Chosen as 'Best' (% of simulations) | | |
|---|---|---|
| True Model | Equally-spaced Experiments | Buzzi-Ferraris and Forzatti Method |
| Terminal | 100.0 | 96.3 |
| Strong penultimate | 100.0 | 100.0 |
| Small penultimate | 96.3 | 100.0 |
| All Models | 98.7 | 98.7 |

more precise reactivity ratio estimates compared with composition data. This leads naturally to a question about which sensors are optimal for making measurements in a particular process.

It is obvious that accurate information about the variables (states) of interest is a key issue in the problems related to estimation, discrimination and process control. It is therefore important to choose the appropriate sensor design which maximizes the information contained in the resulting measurements. The sensor design refers to the type and number of sensors incorporated in a process, their precision and location, and can also be used to explore the utility of a hypothetical sensor.

While Sections 3 and 4 have dealt with issues related to the development of the polymerization simulation model, in this section we present an application of the model, in which it is incorporated into an optimal sensor selection methodology which can help address the above questions for a given process. It should be pointed out that an optimal sensor selection study can only be carried out in a meaningful way if a good process model is available.

The approach which has been taken here involves the use of the Kalman filter. This state estimation technique filters out the measurement noise in order to follow the state trajectory of the process. The filtering mechanism is not arbitrary, but rather consists of the process model combined with available measurements. Hence the Kalman filter combines process data with the process model in an optimal fashion.

Consider the process model in its linear(ized), discretized form:

$$X_{k+1} = \Phi_k X_k + \Delta_k u_k + w_k \qquad (20a)$$

$$y_k = H_k X_k + v_k \qquad (20b)$$

where $X_k$ is the $n \times 1$ state variable vector at time $k$, $u_k$ is the $r \times 1$ manipulated (input) variable vector, $y_k$ the $m \times 1$ measurement vector, $H_k$ the measurement matrix and $w_k$ and $v_k$ are independent Gaussian white noise vectors with zero mean,
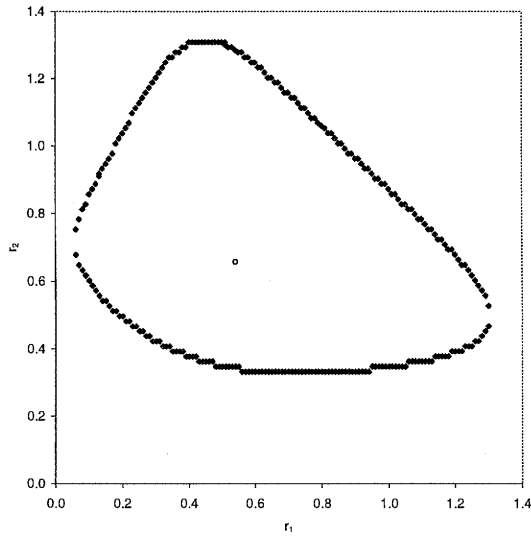
Fig. 7.  The 95% joint confidence region for the the penultimate parameters
         $r_{11}$ and $r_{21}$ after nine experiments. The 'o' represents point estimates.
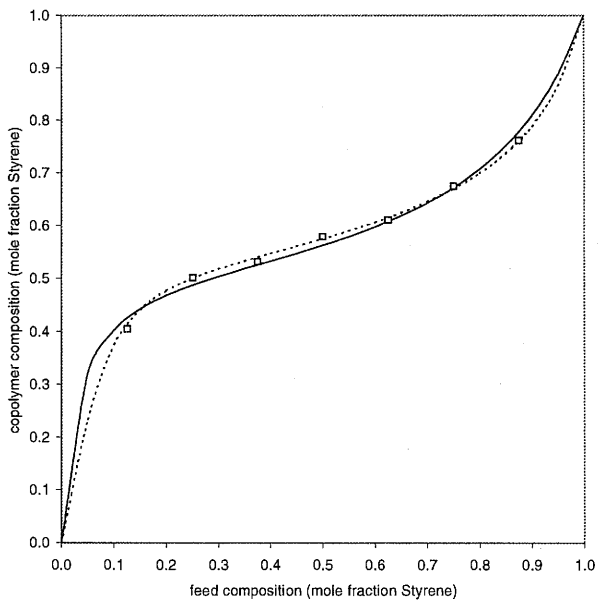


Fig. 8.  The use of equally-spaced experiments for the system styrene/methyl
         methacrylate.

representing the process (model) and measurement noise (uncertainty), respectively. Equation (20) is derived from the copolymerization model described in Section 2. State variables here include moles of initiator, moles of Monomers 1 and 2 in the reacting mixture, moles of monomer incorporated into the polymer, conversion, volume of the reacting mixture, moments of the molecular weight distribution and cumulative triad fractions. Measurements include variables such as conversion, copolymer composition, weight-average molecular weight, triad fractions, polymerization rate and radical concentration. Details describing how the copolymerization model is cast into the Kalman filter form given by eqn. (20) can be found in DeWitte (1996).

Equations (21)–(25) with initial conditions $\hat{X}_0$ and $P_{0/0}$ define the extended Kalman filter (Brown, 1983; Chien and Penlidis, 1990; MacGregor *et al.*, 1986). First the deterministic and stochastic state vectors are predicted by

$$\hat{X}^d_{k+1/k} = \hat{X}^d_{k/k} + \int_{t_k}^{t_{k+1}} f\big(\hat{X}^d(t), u(t), t\big)\, \mathrm{d}t \tag{21a}$$

$$\hat{X}^s_{k+1/k} = \Phi^s \hat{X}^s_{k/k} \tag{21b}$$

where $\hat{X}^d_{k+1/k}$ and $\hat{X}^s_{k+1/k}$ are the one-step ahead predictions for the deterministic and stochastic state vectors, respectively, $\hat{X}^d_{k/k}$ and $\hat{X}^s_{k/k}$ are the corresponding filtered estimates from the previous step and $f(X(t), u(t), t)$ is the right-hand side of the general nonlinear state differential equation description of the process. The inclusion of stochastic states in the Kalman filter formulation is necessary to eliminate offset in the state estimates when chemical processes experience nonstationary stochastic disturbances (MacGregor *et al.*, 1986; Gagnon and MacGregor, 1991). The augmented state vector, composed of both the deterministic and stochastic states, is then used in the following equations:

$$P_{k+1/k} = \Phi_k P_{k/k} \Phi_k^T + R_w \tag{22}$$

$$\hat{X}_{k+1/k+1} = \hat{X}_{k+1/k} + K_k \big(y_{k+1} - h(\hat{X}_{k+1/k}, t)\big) \tag{23}$$

$$P_{k+1/k+1} = P_{k+1/k} - K_k H_{k+1} P_{k+1/k} \tag{24}$$

$$K_k = P_{k+1/k} H_k^T \big(H_k P_{k+1/k} H_k^T + R_v\big)^{-1} \tag{25}$$

where $P_{k+1/k}$ is the covariance matrix for $\hat{X}_{k+1/k}$, $P_{k+1/k+1}$ stands for the covariance matrix for $\hat{X}_{k+1/k+1}$, $K_k$ denotes the Kalman gain matrix, $R_w$ signifies the process noise covariance matrix, $R_v$ denotes the measurement noise covariance matrix and $h(X, t)$ is the (nonlinear) measurement model.

Competing sensor designs can be evaluated by their effect on the computed covariance matrices which give a measure of the precision, or a measure of the quality of information, in the corresponding state estimates (Harris *et al.*, 1980). Equations (22), (24) and (25) are independent of the observations, $y_k$, and can be calculated iteratively until the covariance matrices converge. For completely observable systems with positive definite $P_{0/0}$ both $P_{k+1/k}$ and $P_{k+1/k+1}$ will converge to unique,

steady state, positive definite matrices denoted by $P_{k+1/k}^{\infty}$ and $P_{k+1/k+1}^{\infty}$. The optimal sensor design, then, is that which minimizes a scalar function of $P$. The square root of the determinant of $P$ is the scalar function chosen, because it is scale invariant and proportional to the hypervolume of the approximate joint confidence region of the state estimates. The $D$-optimality criterion is defined as follows:

$$\min D_i = \left(\det\left(P_i^{\infty}\right)\right)^{1/2} \qquad i = 1, 2 \tag{26}$$

where $P_1$ is $P_{k+1/k}$ and $P_2$ is $P_{k+1/k+1}$. $D_2$ is the intuitive choice because it contains information after the state estimate is updated by a new measurement (filtered state), and is the measure we have used in our work.

As an example of the application of this approach we present a case study which examines the effect of initial feed composition ($f_{10}$) on the optimal selection of sensors (note that the subscript 1 refers to styrene). Three initial feed compositions were considered ($f_{10} = 0.3, 0.52, 0.7$) in order to capture different behaviours of the styrene/methyl methacrylate copolymerization. For all simulations in this group of investigations, the high level of $R_w$ (worst case scenario) was used.

For each value of $f_{10}$, the simulation program was run for different sensor scenarios. The outputs from the program were the values of $D_2$ at 5% increments of conversion, up to 25% conversion. Recall that the optimal sensor set is that which minimizes $D_2$.

Typical results from the sensor selection study for $f_{10} = 0.3$ are shown in Fig. 9, where the $D_2$ values are plotted for each of the sensor scenarios in the order of low to high $D_2$, corresponding to the most towards the least optimal sensor set. The numerical symbols plotted correspond to sensor scenarios, which are defined on the abscissa. The plot thus gives the order of optimality of the sensor sets, and compares the relative optimality based on the magnitude of the $D_2$ values.

The approach for guiding the reader in interpreting the plot and determining which sensors are significantly more optimal than the rest is a "scree" plot interpretation (borrowed from principal component analysis), illustrated for 5% conversion in Fig. 9. In this plot, a curve is drawn through the first three groupings of sensor sets, levelling off with the plateau group. The interpretation is that the sensor scenarios which fall on the steep part of the curve are significantly more optimal than the rest. The sensor scenarios falling on the flat part of the curve have more or less the same degree of optimality, and would each give approximately the same amount of information about the system. The sensor scenarios which lie above the flat part of the curve are significantly less optimal than the rest.

The order of optimality in Fig. 9 correlates with the number of measurements in the sensor sets. The more measurements in a sensor set, the more optimal the sensor set is. This is to be expected, since more measurements will give more information about the system. For instance, sensor set (15) is by far the most optimal. It essentially employs 6 measurements: 4 triad fractions, one $k_p$ measurement and one $[R^{\bullet}]$ measurement. $[R^{\bullet}]$ denotes polymer radical concentration and appears as [rad] in the figures. The next most optimal sensor set, (12), has only three measurements: conversion ($x$), copolymer composition ($F_1$), and weight-average molecular weight ($\bar{M}_w$).

Secondly, just examining the sensor pairs, it is immediately evident that the pairs which include the conversion $(x)$ sensor are the two most optimal sensor pairs. This behaviour is also reflected in the order of optimality of the single sensors, where the $x$ sensor on its own is the optimal single sensor. The reason for the importance of the conversion sensor could be that conversion changes at a more rapid rate than the other variables, such as $F_1$, $\bar{M}_w$, $k_p$ and $[R^\bullet]$. These latter variables are fairly constant over the 0–25% conversion range. More information is obtained in the case of conversion, when the state is changing considerably, and thus the signal-to-noise ratio is high. For the other variables, the signal-to-noise ratio is low, and less information about the process is obtained since it is difficult to determine via the respective measurements whether the states are changing or not.
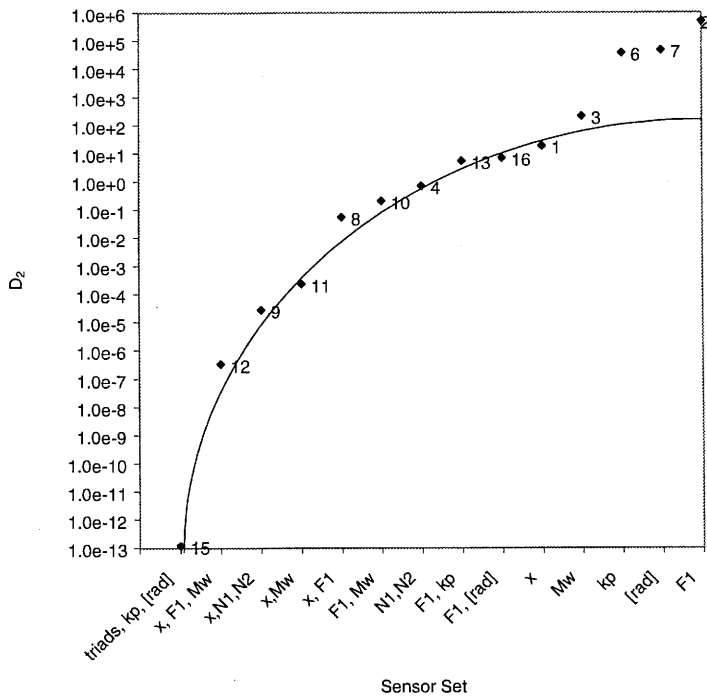


Fig. 9. Optimal order of sensors for styrene/methyl methacrylate based on the Kalman filter technique, $f_{10} = 0.3$, $R_w$: high level, $x = 5\%$.

Additional results for the other two feed mole fractions (see DeWitte, 1996) showed that the selection of optimal sensor sets is not affected by the value of $f_{10}$ or by the conversion level.

Penlidis and Duever (1996) discuss additional case studies including the effect of model uncertainty, measurement precision, including a near errorless $k_p$ measurement, impurity effects and other copolymer systems.

## 6. Concluding Remarks and Future Directions

In this paper, we have shown how appropriate experimental design and estimation methods can assist and enhance the systematic development of a polymer simulation package. As mentioned earlier, the development of this simulator is an ongoing effort which in parallel includes the development of a comprehensive polymerization database. In order to update our polymerization database, we need to address interesting and challenging multiresponse estimation and design problems. The multiresponse estimation problems addressed in this paper have usually involved algebraic equations only. The models we need to address next consist of rather large sets of integro-differential equations and can have a relatively large number of parameters. Our future work in this area includes the development of methods that can address these challenging problems. To do this we are revisiting methods that have been proposed including an investigation into the properties and performance of the determinant method. We are also looking at promising new methods for parameter estimation such as the Gibbs Sampler, amoung others.

There is no doubt that the idea of model-aided research and development is maturing and as our process models improve, they allow us to address a number of interesting problems. We have illustrated this using the problem of sensor selection. One important application of this methodology lies in the fact that it can assist in the identification of promising new sensors.

## Acknowledgements

## References

Aerdts A.M. (1993): *Microstructure of Styrene Methyl Methacrylate Copolymers Grafted onto Polybutadiene Seeds.* — Ph.D. Thesis, Technische Universitaet Eindhoven, The Netherlands.

Behnken D.W. (1964): *Estimation of copolymer reactivity ratios: An example of nonlinear estimation.* — J. Poly. Sci.: A, Vol.2, pp.645–668.

Box G.E.P. and Draper N.R. (1965): *The Bayesian estimation of common parameters from several responses.* — Biometrika, Vol.52, pp.355–365.

Brown, R.G. (1983): *Introduction to Random Signal Analysis and Kalman Filtering.* — Toronto: John Wiley.

Burke A.L. (1994): *Model Discrimination Techniques for the Modelling of Copolymerization Processes.* — Ph.D. Thesis, Department of Chemical Engineering, University of Waterloo, Waterloo, Canada.

Burke A.L., Duever T.A. and Penlidis A. (1993): *Revisiting the design of experiments for copolymer reactivity ratio estimation.* — J. Polym. Sci., Polym. Chem., Vol.31, pp.3065–3072.

Burke A.L., Duever T.A. and Penlidis A. (1994a): *Model discrimation via designed experiments: Discriminating between the terminal and penultimate models on the basis of composition data.* — Macromolecules, Vol.27, pp.386–399.

Burke A.L., Duever T.A. and Penlidis A. (1994b): *Model discrimation via designed experiments: Discriminating between the terminal and penultimate models based on triad fraction data.* — Macromol. Theory Simul., Vol.3, pp.1005–1031.

Burke A.L., Duever T.A. and Penlidis A. (1995): *Model discrimation via designed·experiments: Discriminating between the terminal and penultimate models based on rate data.* — Chem. Eng. Sci., Vol.50, No.10, pp.1619–1634.

Burke A.L., Duever T.A. and Penlidis A. (1996): *An experimental verification of statistical discrimination between the terminal and penultimate copolymerization models.* – J. Poly Sci.: Polym. Chem., Vol.34, pp.2665–2678.

Burke A.L., Duever T.A. and Penlidis A. (1998): *Discriminating between the terminal and penultimate models using designed experiments: An overview.* — Ind. Eng. Chem., (in press).

Buzzi-Ferraris G. and Forzatti P. (1983): *A new sequential experimental design procedure for discriminating amoung rival models.* — Chem. Eng. Sci., Vol.38, No.2, pp.225–232.

Chien D.C.H. and Penlidis A. (1990): *On-line sensors for polymerization reactors.* — JMS–Rev. Macromol. Chem. Phys., Vol.C30, No.1, pp.1–42.

DeWitte M.K. (1996): *Optimal Sensor Selection Methodology for Chemical Processes.* — M.A.Sc. Thesis, Department of Chemical Engineering, University of Waterloo, Waterloo, Canada.

Draper N.R. and Hunter W.G. (1966): *Design of experiments for parameter estimation in multiresponse situations.* — Biometrika, Vol.53, Nos.3 and 4, pp.525–533.

Dube M.A., Sanayei R.A., Penlidis A., O'Driscoll K.F. and Reilly P.M. (1990): *A microcomputer program for estimation of copolymerization reactivity ratios.* — J. Polym. Sci.: A: Polym. Chem., Vol.29, pp.703–708.

Gagnon L. and MacGregor J.F. (1991): *State estimation for continuous emulsion polymerization.* — Can. J. Chem. Eng., Vol.69, pp.648–656.

Gao J. and Penlidis A. (1996): *A comprehensive simulator/ database package for reviewing free-radical homopolymerizations.* — J.M.S. Rev. Macromol. Chem. Phys., Vol.C35, No.2, pp.149–404.

Harris T.J., MacGregor J.F. and Wright J.D. (1980): *Optimal sensor location with an application to a packed bed tubular reactor.* — AIChE J., Vol.41, No.11, pp.2451–2464.

Hill D.J.T., O'Donnell J.H. and O'Sullivan P.W. (1982): *Analysis of the mechanisms of copolymerization of styrene/ acrylonitrile.* — Macromolecules, Vol.15, pp.960–966.

Hsiang T. and Reilly P.M. (1971): *A practical method for discriminating amoung mechanistic models.* — Can. J. Chem. Eng., Vol.49, pp.865–871.

MacGregor J.F., Kozub D.J., Penlidis A. and Hamielec A.E. (1986): *State estimation for polymerization reactors.* — Proc. IFAC Intern. Symp. *Dynamics and Control for Chemical Reactors and Distillation Columns DYCORD 86*, Bournemouth, U.K., pp.147–152.

Maxwell I.A., Aerdts A.M. and German A.L. (1993): *Free radical copolymerization: An NMR investigation of current kinetic models.* — Macromolecules, Vol.26, pp.1956–1964.

Penlidis A. (1994): *Polymer reaction engineering: From reaction kinetics to polymer reactor control.* — Can. J. Chem. Eng., Vol.72, pp.385–391.

Penlidis A. and Duever T.A. (1996): *Optimal sensor selection for copolymerization processes.* — Macromol. Symp., Vol.111, pp.195–207.

Reilly P.M. (1970): *Statistical methods in model discrimination.* — Can. J. Chem. Eng., Vol.48, pp.168–173.

Rossignoli P.J. and Duever T.A. (1995): *The estimation of copolymer reactivity ratios: A review and case studies using the error-in-variables model and nonlinear least squares.* — Polymer Reaction Engineering, Vol.3, No.4, pp.361–395.

Tidwell P.W. and Mortimer G.A. (1965): *An improved method of calculating copolymerization reactivity ratios.* — J. Polym. Sci., Polym. Chem., Vol.3, pp.369–387.

Tidwell P.W. and Mortimer G.A. (1970): *Science of determining copolymerization reactivity ratios.* — J. Macromol. Sci.-Revs. Macromol. Chem., Vol.C4, No.2, pp.281–312.